

## BEHAVIOUR OF STEEP CLAY EMBANKMENTS REINFORCED WITH A NON-WOVEN GEOTEXTILE HAVING VARIOUS FACE STRUCTURES

TATSUOKA, F; TAMURA, Y  
TOKYU CONSTRUCTION CO LTD  
JAPAN

NAKAMURA, K  
INSTITUTE OF INDUSTRIAL SCIENCE, UNIVERSITY OF TOKYO  
JAPAN

IWASAKI, K  
MITSUI PETROCHEMICAL INDUSTRIES LTD  
JAPAN

YAMAUCHI, H  
PENTA-OCEAN CONSTRUCTION CO LTD  
JAPAN

### 1. INTRODUCTION

It has been demonstrated in the previous papers (1), (2) and the companion paper (3) that stable steep clay slopes can be constructed by using horizontally-placed non-woven geotextile sheets in spite of their relatively low tensile stiffness. The importance of adequate face structures for preventing local compressional failure of the soil near the slope face has also been demonstrated. However, the roles of the face structures cannot be limited to the above.

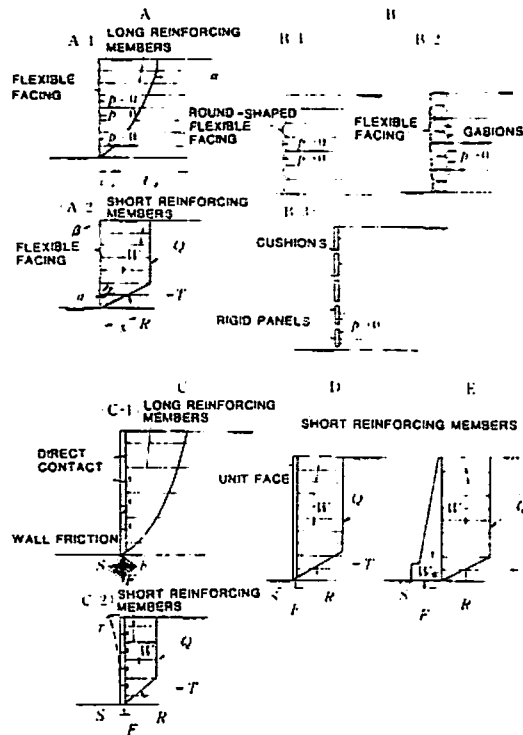
In this paper, the roles of face structures for steep clay slopes reinforced with a geotextile will be classified and defined. Then, they will be discussed based on the behavior of two test clay embankments reinforced with a non-woven geotextile having various face structures.

### 2. ROLES OF FACE STRUCTURES (IN GENERAL)

Fig.1 illustrates various face structures, classified in terms of the following four functions:

(1) Local rigidity for providing the lateral confinement, represented by the earth pressure  $p$ , to the soil next to the slope face in order to avoid its local compressional failure.

Wall A has a flexible slope face such as a geotextile sheet covering a



FUNCTION	FACING TYPE	A	B-1	B-2	B-3	C	D	E
LOCAL RIGIDITY		×	1	2	3	4	○	○
OVERALL AXIAL RIGIDITY		×		×		○	○	○
OVERALL BENDING RIGIDITY		×		×		×	○	○
GRAVITY REGISTANCE		×		×		×	×	○

Note: 1) has not this function.  
2) has this function only to a limited extent.  
3) has this function to a large extent.  
4) has this function sufficiently.

Fig.1. Illustrations of various facing structures and their functions.

D1-5: DISPLACEMENT TRANSDUCERS  
S1-7: DISPLACEMENT TRANSDUCERS FOR SETTLEMENT  
E1-16: TENSILE STRAIN GAGES FOR GEOTEXTILES  
P1-5: EARTH PRESSURE CELLS  
U1-6: TIPS FOR POREWATER PRESSURE  
B1-9: REFERENCE POINTS

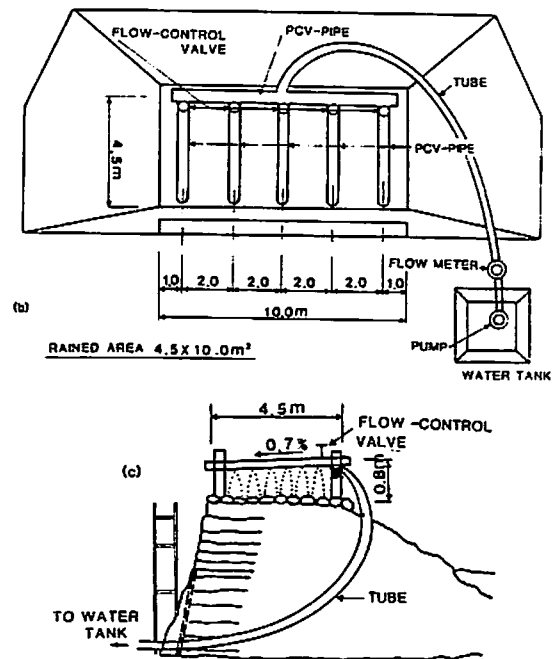
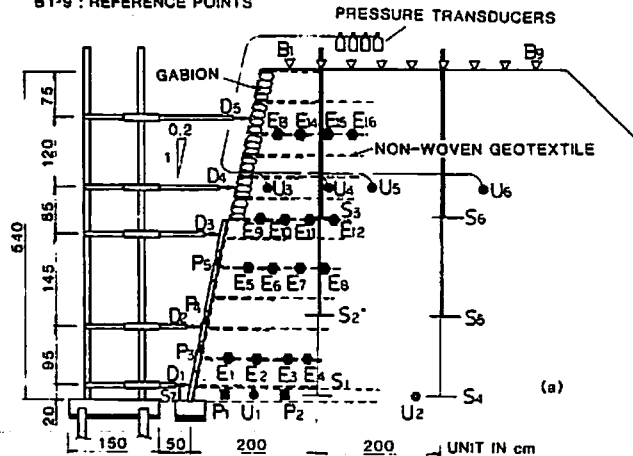


Fig.4. (a) Cross-section, and (b) and (c) arrangements for artificial rainfall (Kami-Onda Embankment).

Fig.2. Possible failure mechanism in a slope reinforced.

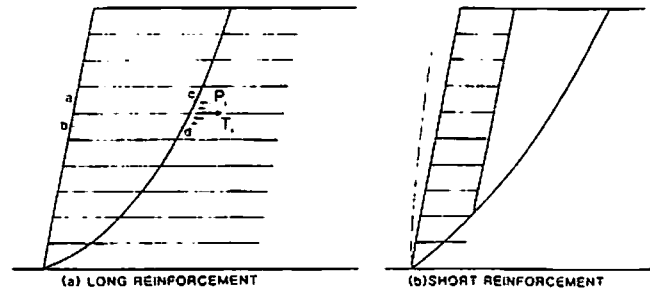
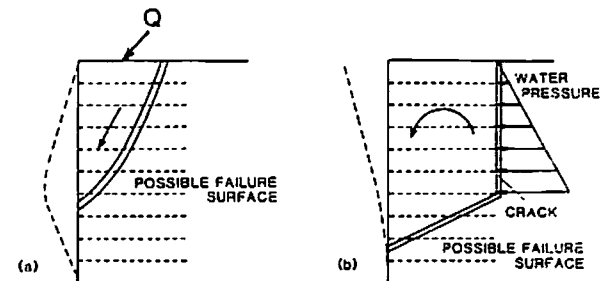


Fig.3.

Possible failure mechanisms for slopes reinforced with short reinforcing members having facing structures without overall bending rigidity.



flat slope face of soil. Apparently, this kind of face structure lacks this function. A relatively large compression may occur locally in the soil near the slope face, especially near the toe, by further filling and loading. This kind of deformation has been observed in Embankment I (see Fig.8 of the paper (2) and Fig.3 of the companion paper (3)).

Wall B-1, which has a rounded flexible face structure of, for example, a metal skin or a geotextile sheet. This kind of face structure has various degrees of this local rigidity. However, this kind of face structure may have the following two disadvantages: (a) It is not easy to compact the soil next to the face structure, accommodating to the rounded shape of the face, thus the degree of compaction may be insufficient. (b) If the initial shape of face is not enough circular, a further compression of the face may take place until a sufficient earth pressure  $p$  is activated.

Wall B-2 has gabions at the face. This face may have a better local rigidity than the flexible face of Wall B-1, if the gabions have been well compressed vertically when placed. This method has been successively used for Embankment II (1)-(3).

Wall B-3 has rigid panels (for example, precast concrete panels). This face structure has a better local rigidity than that of Wall B-2. For the Reinforced Earth retaining wall, a cushion is placed between the upper and lower adjacent precast concrete panels in order that for not damaging the connection between the panel and the reinforcing members the panels can settle down in accordance with possible compression of the back fill. Furthermore, the foundation supporting the face structure may settle down. In such two cases as above, the wall friction may not be mobilized. This means that, from the equilibrium of forces, the shear stresses on horizontal surfaces, for example  $\overline{ac}$  and  $\overline{bd}$  in Fig.2a, are not sufficiently mobilized. Consequently, it is a safe-side design method to consider, as employed in the present practical design method for the Reinforced Earth retaining wall, that each horizontal earth pressure  $P_i$  working on the intersection of a soil slice including a reinforcement layer is totally resisted by the tensile reinforcement force  $T_i$  working at the intersection. This point has been discussed by Juran and Schlosser (4) and also in the companion paper (3).

When the reinforcements are so short that some of upper reinforcements do not extend beyond the failure surface (Fig.2b), the horizontal earth pressure working on the back surface of the upper soil layers is transmitted to the lower soil layers through shear stresses on horizontal surfaces. Consequently, the shear deformation of the reinforced zone as denoted by

the broken lines in Fig.2b is induced and also overturing of the reinforced zone becomes easier to occur.

(2) Overall axial rigidity for supporting a part of the weight of back fill, transmitting it to the base ground through the wall friction. By this kind of face rigidity, either the tensile forces in reinforcements are reduced when the reinforcements are sufficiently long with all the reinforcements extending beyond the failure surface, or the shear deformation and the tendency to overturning of the reinforced zone are reduced when the reinforcements are relatively short.

For Wall C, each rigid panel is in contact with the upper and lower adjacent panels and has a rough back face. Furthermore, panels are supported by a deep foundation or a stiff base ground so that a vertical force, as denoted as  $F$  in Fig.1, is mobilized at the bottom of the face structure. A shear force, as denoted as  $S$  in Fig.1, may be mobilized correspondingly, which also increases the stability of the wall.

When vertical compression in the soil behind the face structure is too large, the connection of the reinforcement to the back face of the face structure may be damaged. To avoid this problem, either the soil behind the wall should be well compacted and/or incompressive granular materials are used near the face structure, or some structural measures should be taken for permitting the reinforcing members to slide relative to the facing; these may be (a) the use of sliding connection as used by Jones (5), or (b) the use of some buffers such as gabions between the facing and the reinforcing members. The both methods were used in the present study (see Figs 7 and 8).

(3) Overall bending rigidity: When a load is applied on the crest of the reinforced zone having relatively short reinforcing members such as Wall C as shown in Fig.3a, or when the water pressure in a crack as shown in Fig.3b is applied to the reinforced zone, the facing may be bent, as denoted by broken curves, associated with a shear failure within the reinforced zone. The manner of the bending of the facing may be different as shown in Fig.3, depending on the loading pattern. In any case, Wall D, having a facing with an overall bending rigidity, has a larger degree of stability than Wall C. A series of single precast concrete plate having a length equal to the total wall height or a shot-crete skin reinforced with wire mesh have this kind of overall bending rigidity.

(4) Gravity resistance: When reinforcing members are connected to the back face of a gravity-type wall, the dimension of the wall can be reduced

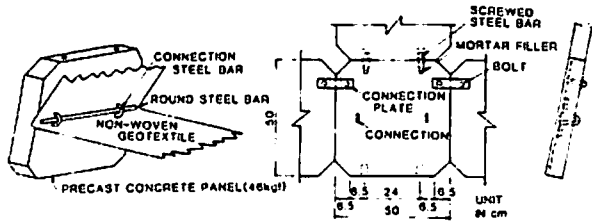


Fig.5. Detailed structure of precast concrete panel.

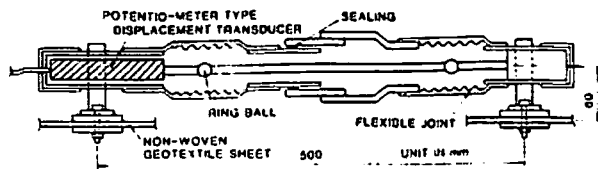


Fig.6. Device for measuring tensile strains in geotextile sheets.

Table 1. Properties of soil used for Kami-Onda Embankment

Intact :  $w_n=124\%$ ,  $w_l=150\%$ ,  $w_p=75\%$ ,  $PI=75$ ,  $G_s=2.776$ ,  $D_{50}=46\mu m$ ,

At filling (March 1985) :  $w=116\%$ ,  $S_r=83\%$ ,  $\rho_d=0.58g/cm^3$

At demolishing (Jan. 1985) :  $w=123\%$ ,  $S_r=87\%$ ,  $\rho_d=0.58g/cm^3$ ,  $q_c=2\sim4.5kgf/cm^2$

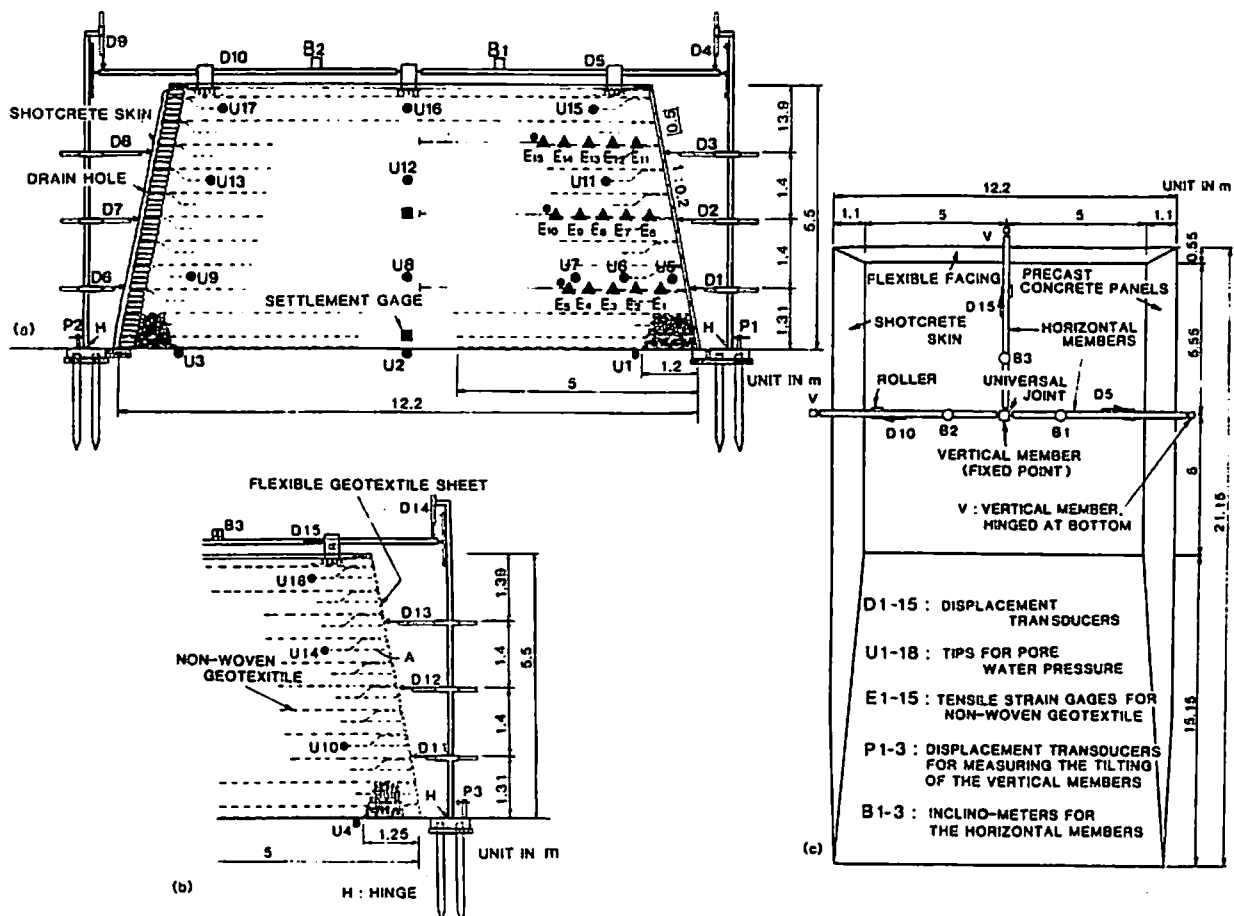


Fig.7. (a) and (b) Cross-sections, and (c) plan of Embankment II at Chiba Experiment Station, Institute of Industrial Science, University of Tokyo.

to a large extent when compared with the case where such reinforcing members are not used. To the best of the authors' knowledges, this type of structure has not been tried.

### 3. CONSTRUCTION OF TEST EMBANKMENTS HAVING FACE STRUCTURES

Based on both the experiences obtained from the behavior of Test Embankments I and II (refer to the companion paper (3)) and the above consideration, the following two test embankments were constructed to investigate the effects of face structure on the stability of steep clay embankments. A volcanic ash clay called Kanto loam as used for Embankments I and II was also used to construct them. The non-woven geotextile used was also similar to the one used for the other embankments (3).

Kami-Onda Embankment (Fig.4) was constructed in March 1985 on a 7m-thick fill of a very soft clay (Kanto loam) near Yokohama City, Kanagawa Prefecture. This embankment had only one test slope. The slope had an initial height of 3m and a slope of 1:0.2. The facing consisted of precast concrete panels (Fig.5). A non-woven geotextile sheet is connected to the back faces of several panels by means of a round steel bar and two steel connections embedded in each panel. This connection method does not allow a geotextile sheet to slide down relative to the panel. This drawback was improved later when used for Embankment III (see Fig.8).

In December 1985, an additional reinforced soil layer, with a height of 2.4m and a slope of 1:0.2, was placed above the existing slope as a load to the existing fill. Then, a heavy artificial rainfall, equivalent to as much as 620mm of rainfall over a period of four days, was applied from the crest of the fill to examine the resistance of the embankment against heavy rainfall. In order to simulate natural rainfall, water was pluviated from many small holes made on four pipes located on the crest of the fill (Fig.4c). While the slope experienced a considerable displacement under the artificial rainfall, its overall stability was maintained. Then, after 20 days, the embankment was demolished.

The physical properties of the intact Kanto loam was slightly different from that used for Embankments I, II and III (see Table 1). The system for measuring displacements, pore pressures and so on was similar as for Embankments I and II. Tensile strains of non-woven geotextile sheets, averaged over a gage length of 50cm, were obtained by measuring the elongation of the gage length by means of the device shown in Fig.6. The potentiometer type displacement transducer has a capacity of 5cm and is

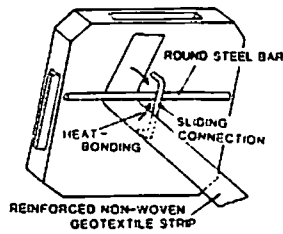


Fig.8. Detailed structure of precast concrete panel.

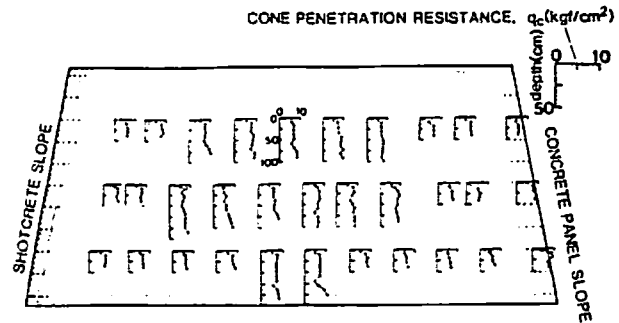


Fig.9. Cone penetration resistances of soils as compacted, Embankment II.

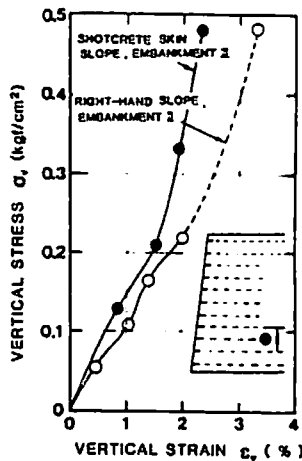


Fig.10. Compression of a soil layer at the slope face having gabions during filling.

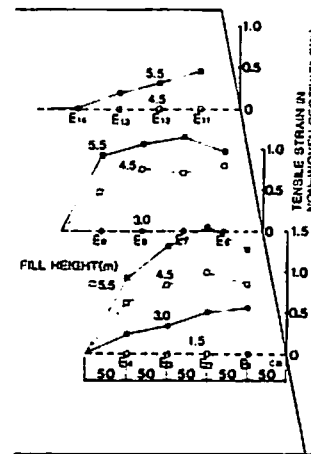


Fig.11. Tensile strains in geotextile sheets in concrete panel slope during filling.

activated by 5V DC input. The locations of the center of the device are indicated by  $E_1$  through  $E_{16}$  in Fig.4a.

A spun-bonded 100% polypropylene non-woven geotextile having a nominal mass per unit area of  $400\text{g/m}^2$  was used.

Embankment III (Fig.7) was constructed in October 1986 using the soil obtained by demolishing Embankments I and II (see also Fig.1 of the companion paper (3)). It has three test slopes having a nominal slope of 1:0.2 and a height of 5.5m. A spun-bond 100% polypropylene non-woven geotextile having a nominal mass per unit area of  $300\text{g/m}^2$  was used as reinforcing sheets as for Embankment II. The lowest two sheets were made longer as 5m in order to drain better the soil at the lower levels in the embankment, since the

shear strength of the soil there has a large influence on the stability of the slope, as indicated by the stability analysis as presented in the companion paper (3). The top two non-woven geotextile sheets were also made longer as 5m, in order to prevent the possible development of cracks from the crest and also to increase the resistance of geotextile against overturning.

A mass of crushed gravel was placed near the toe in order to collect water effectively from the interior of embankment and also to increase the resistance against overturning by increasing the strength of the toe of the slope. The three test slopes have three different faces as follows:

(1) Precast-concrete panel face (as Wall C-2 in Fig.1). A face structure, consisting of precast concrete panels as shown in Fig.8, was placed on a foundation which had been made for not allowing its settlement. Each panel has a dimension of 50cm×50cm×5cm and a weight of 34kgf, which was made lighter than the ones used for Kami-Onda Embankment for easier manual handling. Further, projections and grooves were made at its four edge surfaces for easier connection to the adjacent panels. A 10cm-wide strip of non-woven geotextile reinforced with a polypropylene sheet having a high tensile stiffness was connected to each panel by means of a round steel bar and a sliding connection embedded in the panel (Fig.8). The reinforced strip geotextile has a yielding load of 1.18 tonf/m at a tensile strain of 4.7%. The sliding connections allow the settlement of the strip relative to the face. One end of the strip was heat-bonded to another part of the strip over 15cm to make a ring to hook the steel bar. The strip was placed between two planar non-woven geotextile sheets so that the geotextile sheets are to be connected to the concrete panels.

Strains in geotextile sheets were measured only in this slope. The increase of the distance between the back face of the reinforced zone and the center line of the embankment was measured by means of E5, E10 and E15 (see Fig.7a).

(2) Shotcrete skin face (as Wall D in Fig.1). After the slope had been completed by using gabions at the face as the slopes of Embankment II, a skin of shotcrete reinforced with wire mesh, having a thickness of about 8cm, was placed on the existing slope face as shown in Fig.7a. The shotcrete skin was anchored with 10cm-wide reinforced non-geotextile strips as mentioned above to the main body of the embankment. Drain holes were placed as needed. It was expected for the gabions to work as buffers for possible relative settlements between the shotcrete skin and the embankment.



(3) Flexible face (as Wall A in Fig.1). The flat slope faces of soil were made and they were wrapped around with geotextile sheets round the soil at the face (Fig.7b). No structural measures was used. A thin non-woven geotextile sheet having a nominal thickness of 1.5mm (which is a half of the non-woven geotextile used as the reinforcing material) and a length of 1m, as denoted by the letter A in Fig.7b, was placed horizontal at the intermediate height of each soil layer for better compaction of the soil near the face. This slope was expected to exhibit the poorest performance among the three slopes, providing a good evidence for the importance of face structural measures for such steep clay slopes.

The main body of the embankment was compacted by a heavy compaction plant with a weight of 12tf. A light compaction plant with a weight of 90 kgf was used to compact the soil within about 80cm from the slope face. By this mechanical compaction, the soil near the face was well compacted, as seen from such a result shown in Fig.9 as that the cone penetration resistances near the face were almost the same as those for the main body of the embankment. The average dry weight and the water content of the soil as compacted were  $0.6\text{tf/m}^3$  and 110%, which are very similar as for Embankment II (see Table 1 of the companion paper (3)).

Fig.10 shows the relationship between the overburden and the vertical compressional strain at the slope face in a soil layer in the slope constructed using gabions as indicated in the inset figure, observed during filling. The shape of the curve resembles the one under the one-dimensional compression of soil in the sense that the rate of axial compression decreases as the overburden increases. This implies that the geotextile restrained the horizontal tensile strains in the soil. It may also be seen that the vertical compression of soil near the face is smaller for this slope than that for Embankment II, where manual compaction was employed near the slope face.

Fig.11 shows the tensile strains in the non-woven geotextile sheets for the concrete panel slope which occurred during further filling over each soil layer. It may be seen that the geotextile functioned as a tensile reinforcement during filling. These data also suggest that earth pressures were activated at the back face of the facing, indicating that the precast concrete panels confined the back fill.

All measured quantities were recorded automatically by means of a micro-computer as used for Embankment II.

#### 4. BEHAVIOR OF KAMI-ONDA EMBANKMENT

Fig.12 shows (a) the horizontal outwards displacements at the slope face, and the settlements, earth pressures and pore water pressures at several points in the interior of the embankment, and (b) tensile strains in the geotextile sheets, where the record from 6 April through 26 November, 1985 has been omitted for simplicity. Fig.13 shows the distribution of tensile strains in the geotextile sheets. The detailed behavior during the artificial rainfall is given in Figs.14 and 15. Note that the pore pressures U1 and U2, as shown in Fig.14d, were already zero (U1) or positive (U2) before the artificial rainfall, since the measuring points were already at the ground water level (U1) or below it (U2). The cross-section observed at dismantling is shown in Fig.16. The following points may be seen from the figures:

(1) The lower fill of the embankment had been very stable before constructing the upper part. It exhibited only slight deformations under the effects of the upper part, and had become very stable again during the subsequent period. It exhibited, however, relatively large deformations by the artificial rainfall, but did not lose the overall stability. This result shows that a measures against heavy rainfall may be very important, even more than that against loading at the crest.

(2) During the life time of the embankment, the underlying soft fill was compressed considerably (see Fig.12a); i.e., the back face of the reinforced zone settled down about 40cm finally. It is to be noted that the embankment and the face structure deformed according to the settlement, without showing any structural damage. However, it was found that since the geotextile sheets could not slide relative to the face, the settlement of geotextile sheets was smaller near the face; i.e., the level of geotextile sheets became higher near the face. It resulted in the decrease in the drainage ability of the geotextile.

(3) The major part of the displacement of the slope was the rotation about the toe, with the reinforced zone behaving like a monolith. This point is seen from Fig.12a of the companion paper (3) and also from Fig.16; i.e., cracks were observed only in the unreinforced zone just behind the reinforced zone. This point can be seen further from Fig.17, which shows that only a part of the horizontal displacement at the slope face can be attributed to be the elongation of the reinforced zone. Such behavior as above is characteristics for short geotextile sheets.

(4) Tensile strains in the geotextile sheets increased according to the deformation of embankment. The distribution of the strain (Fig.13) shows

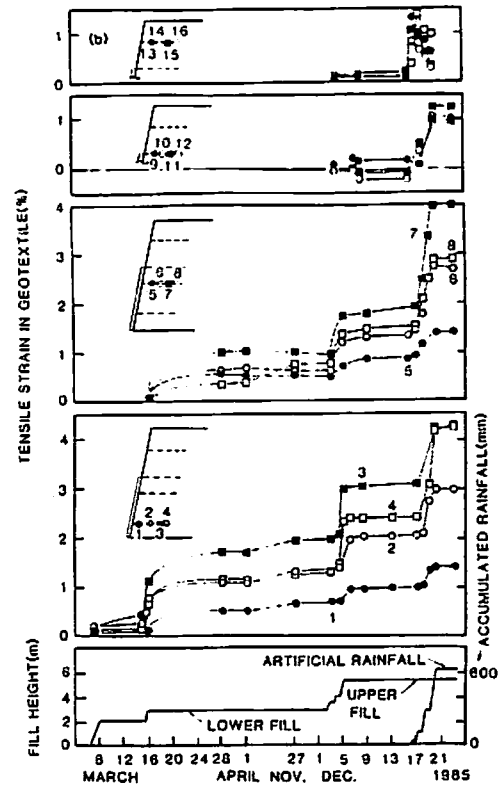
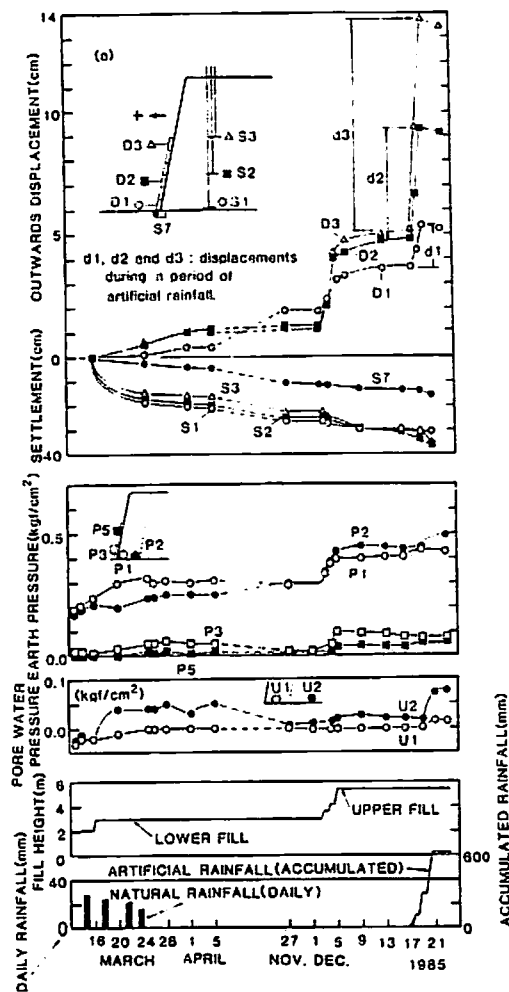
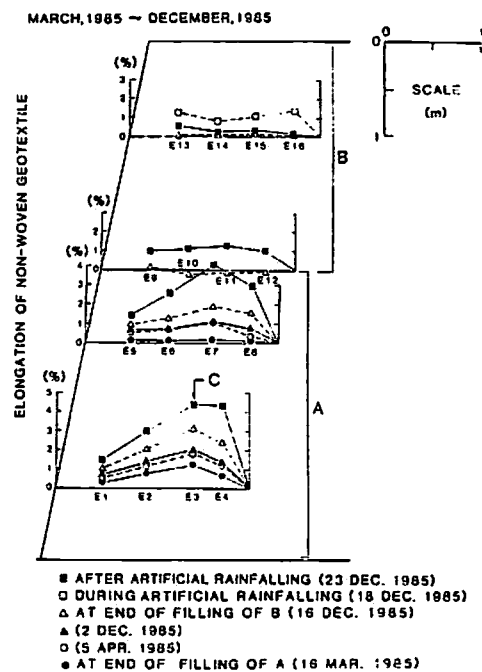


Fig.12. Post-construction behavior of the lower fill of Kami-Onda Embankment.

Fig.13. Distribution of tensile strains in geotextile sheets in Kami-Onda Embankment.



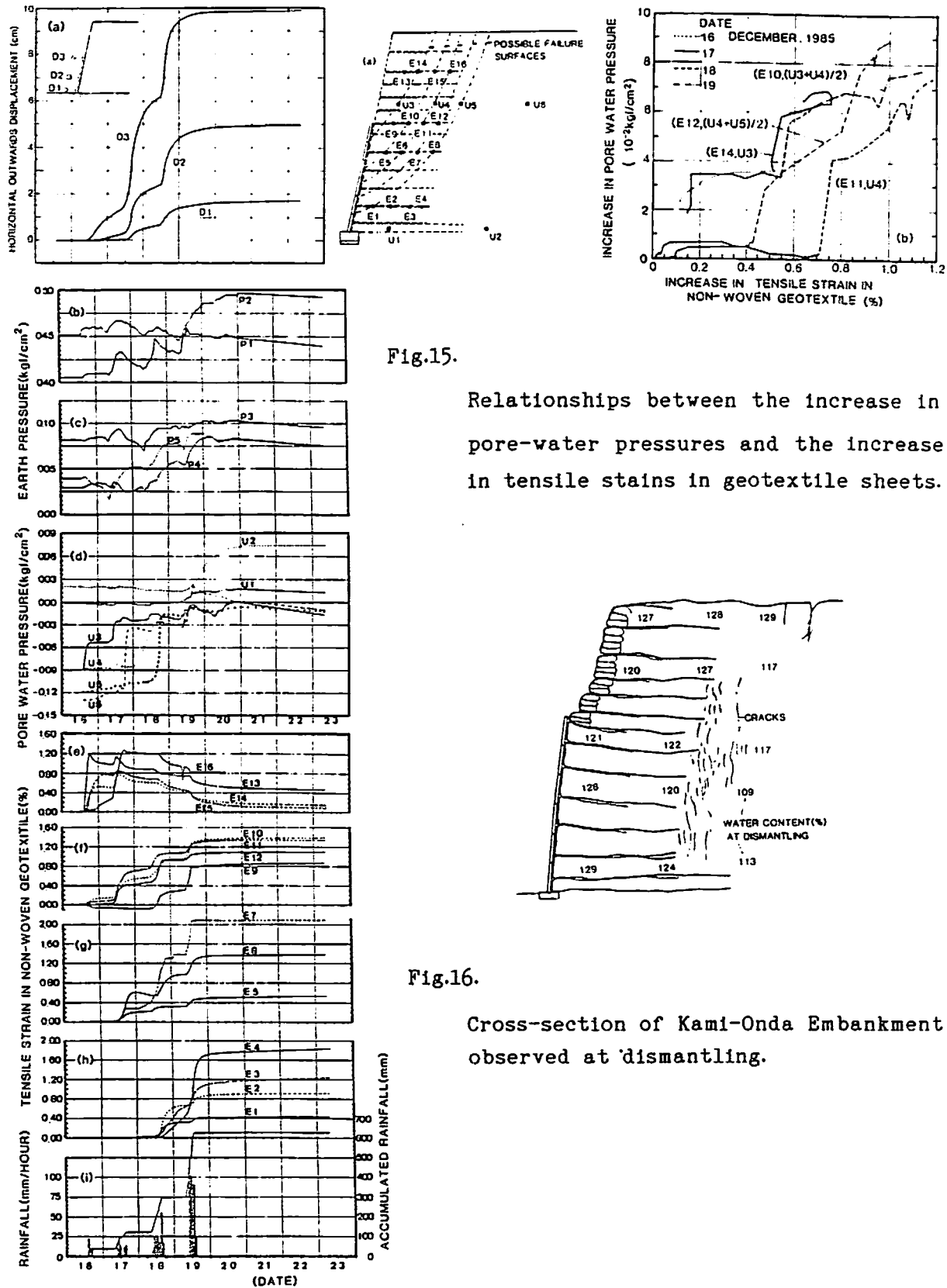


Fig.15.

Relationships between the increase in pore-water pressures and the increase in tensile stains in geotextile sheets.

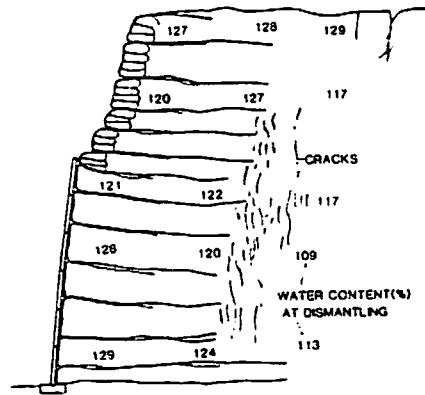


Fig.16.

Cross-section of Kami-Onda Embankment observed at dismantling.

Fig.14. Behavior of Kami-Onda Embankment during a period of artificial rainfall.

that the geotextile sheets functioned as a tensile reinforcing material.

As shown in Fig.18, the rate of creep elongation of the non-woven geotextile decreased at a fast rate after the construction of the lower fill; i.e., until 200 days after the construction, the creep strain rate has decreased to as small as about  $10^{-3}$  %/day, without showing a sign of the increase in the creep strain rate in future. This behavior is well in accordance with such long-term behavior of Embankments I and II as that the creep rate of horizontal outwards displacements at the slope faces in the second and subsequent years were negligible (refer to the papers (1) and (2)). This phenomenon may be due to that the geotextile sheets receive a sustained

Fig.17. Relationships of horizontal outwards displacement between slope face and back face of reinforced zone, Kami-Onda Embankment.

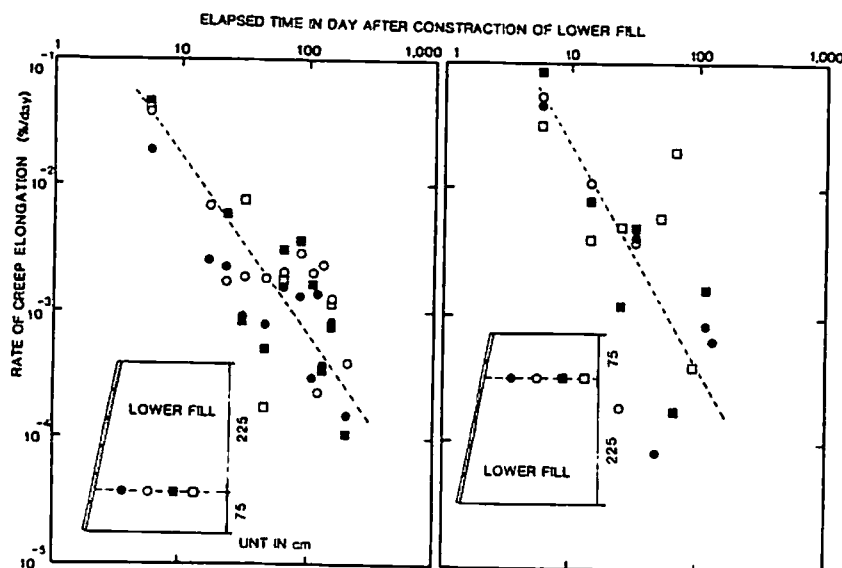
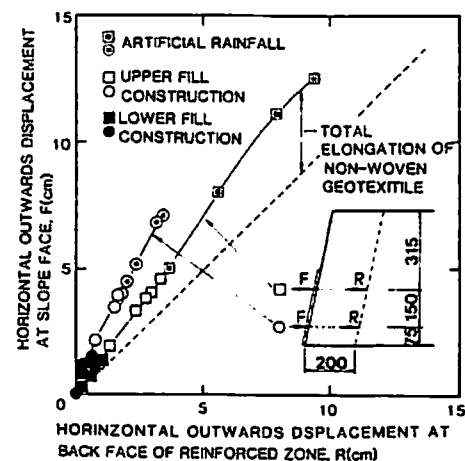


Fig.18 Creep rate of tensile strain in non-woven geotextile sheets used in the lower fill of Kami-Onda Embankment.

load which is smaller than a larger load working only for a short duration on the occasion of heavy rainfall. It follows that the creep deformation of non-woven geotextiles may not be a critical factor when used as for the test embankments constructed in this investigation. This point is discussed also in the previous paper (2).

(5) Since relatively short geotextile sheets were used, the upper part of the sheets may not have extended beyond the failure surface as illustrated in Fig.2b. It seems, therefore, that a large part of the earth pressure working on the back face of the reinforced zone was resisted by the several lower sheets, as may be seen from the amount and distribution of strains in the geotextile (Fig.13). It may be seen from Fig.13 that the length extending the potential failure surface in the lowest sheet is as small as of the order of 30-60cm. However, this length seems sufficient since the calculated mobilized angle of friction  $\phi_\mu$  between the geotextile surface and the soil is only  $2.5^\circ$  or less. The required anchoring length for mobilizing the pull-out resistance equal to the tensile force is only of the order of 10cm if  $\phi_\mu=30^\circ$  can be mobilized. This is a characteristics feature for the planar geotextiles used as reinforcing sheets when compared with strip metal reinforcing members.

(6) The deformation of the slope during a period of artificial rainfall can be clearly attributed to the reduction in the suction and further the increase in the positive pore water pressure caused by the artificial rainfall. The increase in the pore water pressure started earlier at the higher places closer to the crest (i.e., closer to the source of pore water). Fig.15b shows the relationships between the change in the pore water pressure and the change in the tensile strain in the geotextile sheet, caused by the artificial rainfall. Both values of the data for each relationship were measured at closer points located near the same possible failure surface as shown in Fig.15a. It may be seen clearly that the tensile strains in the geotextile sheets increased in accordance with the increase in the pore water pressure.

The overall stability for the horizontal force and moment of the slope was examined using a limit equilibrium method based on a two-part wedge failure mechanism, which is described in detail in the companion paper (3). The results of the analyses are well in accordance with the actual behavior. Both the actual behavior and the analytical result showed (a) a similar failure mechanism; i.e., overturning of the reinforced zone like a monolith about its toe, and (b) large effects of the suction and the pore water

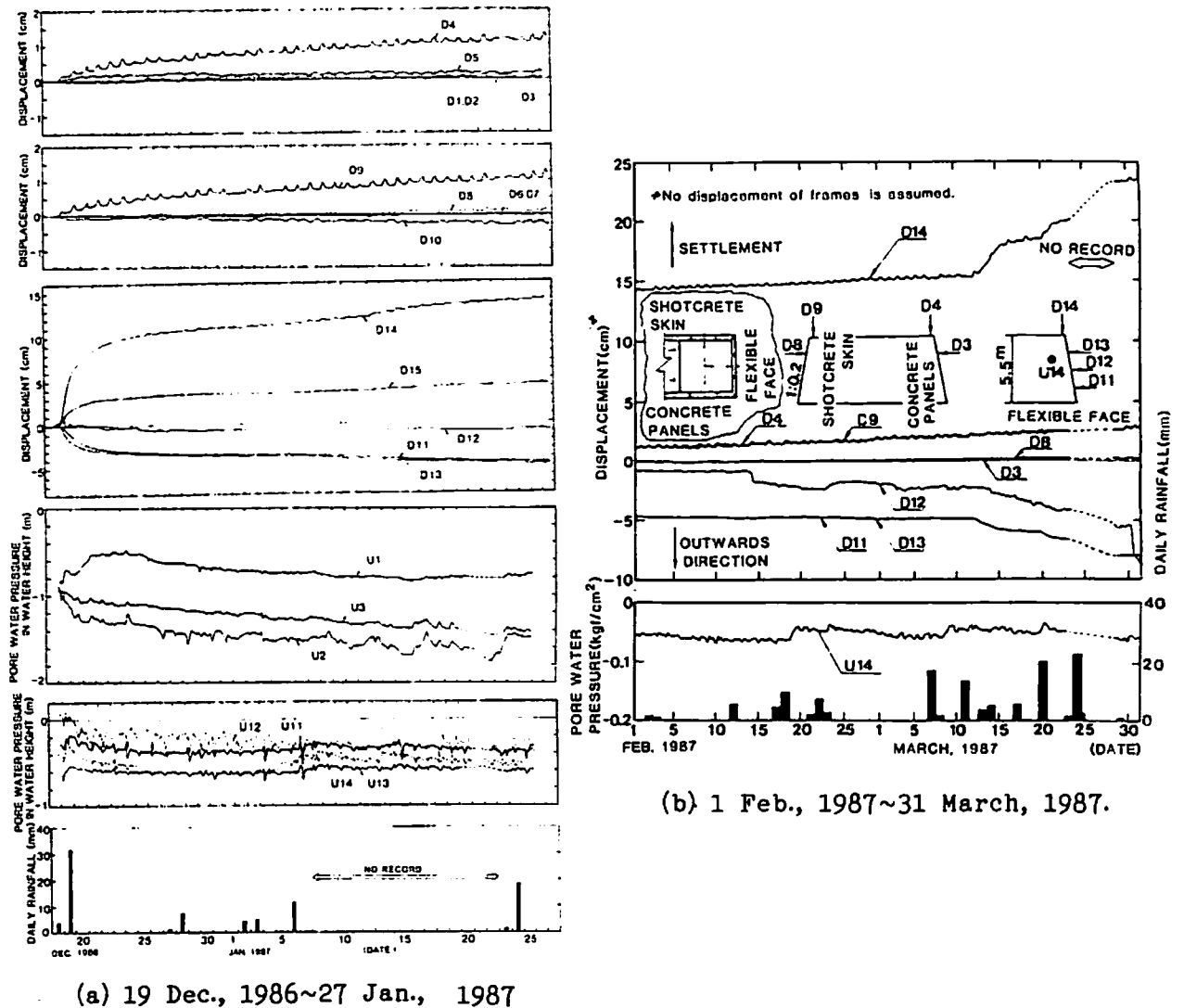
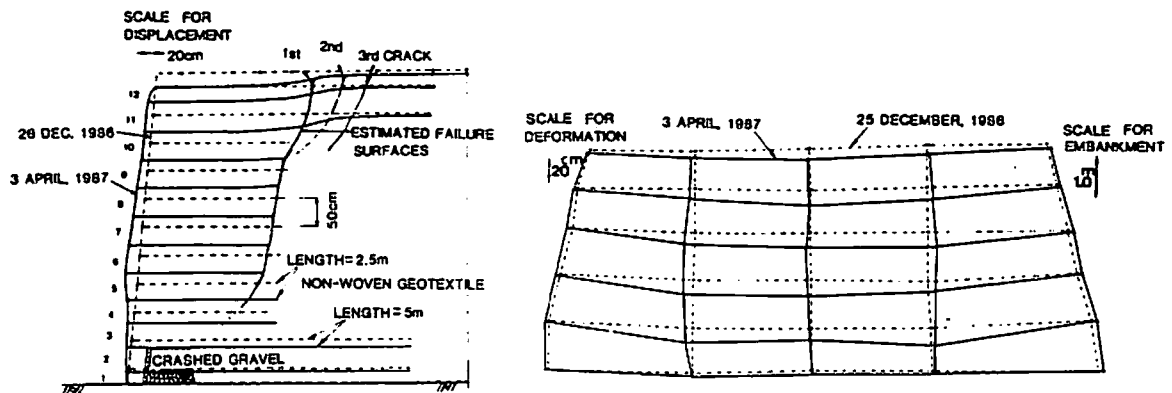


Fig.19. Post-construction behavior of Embankment III.



pressure on the overall stability.

Summarizing the behavior described above, it can be considered that such steep clay slopes reinforced with a non-woven geotextile having a face structure of precast concrete panels, as the lower fill with a height  $H_0$  of 3m of Kami-Onda Embankment, can be constructed also in practice.

#### 5. BEHAVIOR OF EMBANKMENT III

The post construction behavior of Embankment III has indicated clearly the importance of the face structure having (a) local rigidity or (b) local rigidity plus overall axial rigidity for the stability of steep clay embankments reinforced with a geotextile. As seen from Figs 19 and 20, the displacements of the flexible face were much larger than those of the other two faces, the one having gabions and a shot-crete skin and the other one having precast concrete panels. The displacements of these two faces were very small. In particular, it is to be noted that the horizontal outwards displacements at the crest (D3 and D8), which are the good indicator of the instability of the steep slopes, were almost negligible.

The authors considered based on the observed deformations at the flexible slope face that the large deformation of the slope as shown in Fig.20 is due largely to the local vertical compressional failure of the soil near the slope face and an associated sliding failure as illustrated in Fig.20a. This result together with the similar behavior of the left-hand slope of Embankment I (see Fig.3 of the companion paper (3)) clearly indicate that such a flexible face should not be used for steep clay slopes in practice, unless a relatively large deformation of slope is allowed.

The observation of this embankment is now continuing. Its long-term behavior will be reported in the future.

#### 6. CONCLUSIONS

The roles of face structures for steep reinforced slopes were classified and discussed in general terms. These roles are sometimes unduly ignored in routine, practical design procedures. The local rigidity, overall axial rigidity, overall bending rigidity and gravity resistance of face structures were defined and their effects on the stability of steep reinforced slopes were discussed.

Two steep clay embankments reinforced with a non-woven geotextile were constructed. The test slopes were (a) two slopes having precast concrete panels, (b) one slope with a shot crete skin reinforced with wire mesh placed on the slope face which had been constructed using gabions, and (c) the other slope having a flexible face constructed as a reference. The slopes having



the face structures (a) and (b) exhibited rather satisfactory behavior. Consequently, similar slopes may be constructed also in practice.

#### 7. ACKNOWLEDGEMENTS

The authors wish to thank our colleagues, Mr. T. Sato, Mr. S. Yamada and Miss M. Torimitsu for their co-operation in this study. This study was partly sponsored by the Ministry of Education and Culture of the Japanese Government.

#### 8. REFERENCES

1. Tatsuoka, F., Yamauchi(Ando), H., Iwasaki, K. and Nakamura, K., "Performance of Clay Test Embankments Reinforced with a Non-Woven Geotextile," Proc. 3rd Int. Conf. Geotextiles, Wien, Vol. II, pp.355-360. 1986.
2. Tatsuoka, F. and Yamauchi, H. (1986), "A Reinforcing Method for Steep Clay Slopes Using a Non-Woven Geotextile," Geotextiles and Geomembranes, 4, pp.241-268, 1986.
3. Yamauchi, H., Tatsuoka, F., Nakamura, K., Tamura, Y. and Iwasaki, K., "Stability of Steep Clay Embankments Reinforced with A Non-Woven Geotextile," Proc. of the Post Vienna Conf. on Geotextiles, Singapore, 1987.
4. Juran, I. and Schlosser, F., "Theoretical Analysis of Failure in Reinforced Earth Structures," Proc. Symp. on Earth Reinforcement, ASCE Annual Convention, Pittsburg, pp.528-555, 1978.
5. Jones, C. J. F. P., "The York Method of Reinforced Earth Construction," ditto, pp.501-527, 1978.